

The Low-Temperature Structures of $\text{Hg}_{3-\delta}\text{SbF}_6$ and $\text{Hg}_{3-\delta}\text{TaF}_6$

BY Z. TUN* AND I. D. BROWN

Institute for Materials Research, McMaster University, Hamilton, Ontario, Canada L8S 4M1

(Received 31 July 1985; accepted 30 October 1985)

Abstract

The Hg chains in both $\text{Hg}_{3-\delta}\text{SbF}_6$ and $\text{Hg}_{3-\delta}\text{TaF}_6$ order below room temperature. Down to about 190 K the ordering results from the interaction between parallel chains. It is short range and is different for the two compounds. Below 190 K both compounds transform to an isostructural long-range-ordered phase which is driven by the interaction between perpendicular chains. The structure of this phase in both compounds has been determined. $\text{Hg}_{3-\delta}\text{SbF}_6$ at 173 K, $\delta = 0.134(1)$, $M_r = 810.6(2)$. It is monoclinic but pseudotetragonal with $I4_1/amd$, $a = 7.655(1)$, $c = 12.558(1)$ Å, $V = 735.9(2)$ Å³, $Z = 4$, $D_x = 7.314(3)$ Mg m⁻³, graphite-monochromated Mo $K\alpha$ radiation, $\lambda = 0.71069$ Å, $\mu = 64.8$ mm⁻¹, $F(000) = 1337.1(3)$. $\text{Hg}_{3-\delta}\text{TaF}_6$ at 150 K is isostructural but has $\delta = 0.142(1)$, $M_r = 868.2(2)$, $a = 7.634(1)$, $c = 12.610(2)$ Å, $V = 734.9(2)$ Å³, $D_x = 7.844(3)$ Mg m⁻³, $\mu = 76.4$ mm⁻¹, $F(000) = 1422.6(3)$. Comparison of the low-temperature structures with those at room temperature shows that the thermal contraction results from the shortening of interatomic distances associated with the weak bonds, with the result that the MF_6 ($M = \text{Sb}, \text{Ta}$) host lattice shrinks more than the Hg chains. Variation of the atomic displacement parameters with temperature indicates that the large librational displacements of the MF_6 ions result from thermal motion rather than static disorder.

Introduction

It has been more than a decade since the discovery of the first compound, $\text{Hg}_{3-\delta}\text{AsF}_6$, that contains infinite chains of metallicly bonded Hg atoms occupying straight tunnels within an incommensurate host lattice of AsF_6^- ions (Brown, Cutforth, Davies, Gillespie, Ireland & Vekris, 1974). This material crystallizes in the tetragonal space group $I4_1/amd$ and has sets of Hg chains related by the 4_1 -screw axis running along both the \mathbf{a}_H and \mathbf{b}_H host-lattice directions. Because of the incommensurability between the atom spacings (d_{Hg}) in the chains and \mathbf{a}_H , and because of the large interchain distances, the interactions

between the chains are weak ($\ll 300$ K) and each chain behaves at room temperature as a one-dimensional liquid (Spal, Chen, Egami, Nigrey & Heeger, 1980). Diffraction from the chains consists of two sets of diffuse scattering sheets at $n(3-\delta)\mathbf{a}_H^*$ and $n(3-\delta)\mathbf{b}_H^*$ where n is $\pm 1, \pm 2, \dots$ but not zero.† At room temperature the intensity distribution of the sheets is almost uniform, indicating that the ordering between the chains is negligible. (See Fig. 1 in Tun & Brown, 1982.)

In $\text{Hg}_{3-\delta}\text{AsF}_6$ the weak interchain interaction manifests itself at lower temperatures by the development of intensity modulations in the diffuse scattering sheets (Hastings, Pouget, Shirane, Heeger, Miro & MacDiarmid, 1977). At first the modulation peaks are broad and can be seen only on the lowest-order sheets ($n = \pm 1$). They are produced by a short-range order between the sets of parallel chains (S phase). As the temperature is reduced below $T_c = 120$ K the broad peaks are suddenly replaced by a set of narrow peaks at different positions. These peaks can be seen not only on the $n = \pm 1$ sheets but, at lower temperatures, also on the higher-order sheets (Pouget, Shirane, Hastings, Heeger, Miro & MacDiarmid, 1978). The narrow peaks which signal a long-range order of the chains (L phase) are attributed to coherent coupling of the two perpendicular sets of chains *via* common reciprocal-lattice points at the intersection of the planes at $n(3-\delta)\mathbf{a}_H^*$ and $n(3-\delta)\mathbf{b}_H^*$ (Axe, 1980).

The isostructural compounds $\text{Hg}_{3-\delta}\text{SbF}_6$, $\text{Hg}_{3-\delta}\text{NbF}_6$ and $\text{Hg}_{3-\delta}\text{TaF}_6$ have since been prepared (Tun & Brown, 1982; Tun, Brown & Ummat, 1984). We have found that at least two of them undergo similar transitions with $T_c = 186.0(5)$ K ($\text{Hg}_{3-\delta}\text{SbF}_6$)‡ and $T_c = 193(3)$ K ($\text{Hg}_{3-\delta}\text{TaF}_6$). It was not possible to obtain crystals of $\text{Hg}_{3-\delta}\text{NbF}_6$ that were suitable for low-temperature studies. Although the structures of all four compounds are known at room temperature, only $\text{Hg}_{3-\delta}\text{AsF}_6$ has been examined below

† From now on, only the chains in the \mathbf{a}_H direction will be considered but similar statements apply also for the chains in the \mathbf{b}_H direction unless otherwise stated.

‡ This measurement was made by neutron diffraction in collaboration with J. D. Axe and G. Shirane at the Brookhaven National Laboratory, New York.

* Present address: Department of Physics, University of Edinburgh, Edinburgh, Scotland.

room temperature. In this paper, we report studies of the ordering of the Hg chains in both *S* and *L* phases as well as the structure of $\text{Hg}_{3-\delta}\text{SbF}_6$ at 173 K and $\text{Hg}_{3-\delta}\text{TaF}_6$ at 150 K.

Experimental details and results

Samples with dimensions $0.16 \times 0.13 \times 0.09$ mm ($\text{Hg}_{3-\delta}\text{SbF}_6$) and $0.2 \times 0.2 \times 0.01$ mm ($\text{Hg}_{3-\delta}\text{TaF}_6$), prepared by Drs K. Morgan and P. Ummat respectively, handled under usual strictly anhydrous conditions. X-ray intensities measured on Nicolet $P2_1$ diffractometer using standard LT1 cold- N_2 gas apparatus to cool samples. Temperature stability and reproducibility tested at various temperatures down to 150 K and found to be within ± 3 K.

(a) Intensity modulation of the diffuse scattering sheets

In order to investigate the ordering of the Hg chains the intensity distribution of the diffuse scattering sheets was examined at various temperatures. Standard 2θ - ω scans at very low scan speed were performed to measure the diffracted intensity at the points $n(3-\delta)\mathbf{a}_H^*$, $m\mathbf{b}_H^*$, $l\mathbf{c}_H^*$, where m was varied from -1.0 to $+1.0$ with steps of 0.1 for $\text{Hg}_{3-\delta}\text{SbF}_6$ and from -0.25 to $+2.25$ with steps of 0.25 for $\text{Hg}_{3-\delta}\text{TaF}_6$.

The results of these measurements carried out on the $l=0$ layer of the $n=1$ sheet are depicted in Figs. 1 and 2. The presence of short-range order above T_c is evident in both compounds by the observation of broad peaks but the position of the peaks in the two compounds is different. As in the case of $\text{Hg}_{3-\delta}\text{AsF}_6$, the peaks from $\text{Hg}_{3-\delta}\text{SbF}_6$ are centred at $m = \pm 0.4$ but have a much weaker amplitude and larger width (compare with Fig. 5 of Pouget *et al.*, 1978). The *S*-phase peaks of $\text{Hg}_{3-\delta}\text{TaF}_6$ are equally weak and broad but are centred at $m = 0$ and 2 . Measurements on the $l=1$ layer of the same sheet also revealed broad peaks but at $m = \pm 0.6$ for $\text{Hg}_{3-\delta}\text{SbF}_6$ and $m = 1$

for $\text{Hg}_{3-\delta}\text{TaF}_6$. In both compounds the intensity distribution on the $n=2$ sheet is uniform even when the temperature is just above T_c and the first-order peaks are at their maximum amplitude.

Figs. 1 and 2 also show the narrow peaks (FWHM = $0.06 \mathbf{a}_H^*$) which are characteristic of the *L* phase. The profile of these peaks along \mathbf{c}_H^* was also checked and was found to be sharp and centred at $l=0$. (The wider peaks seen in Fig. 2 are probably an artifact of the thin plate-like shape of the $\text{Hg}_{3-\delta}\text{TaF}_6$ crystal, since the same crystal gave sharp peaks along the \mathbf{c}_H^* axis.) In both compounds the position of the *L*-phase peaks at $m = 1 \pm \delta$ is identical to that found for $\text{Hg}_{3-\delta}\text{AsF}_6$. A survey of the $l=1$ layer as well as of the $n=2$ sheet revealed peaks that can be indexed as $n(3-\delta)\mathbf{a}_H^*$, $(k \pm n\delta)\mathbf{b}_H^*$, $l\mathbf{c}_H^*$ with $n+k+l = \text{even}$, indicating that the chains are ordered into a body-centred monoclinic cell. *L*-phase peaks from the *b* chains were also examined and were found at $(h \pm n\delta)\mathbf{a}_H^*$, $n(3-\delta)\mathbf{b}_H^*$, $l\mathbf{c}_H^*$ with $h+n+l = \text{even}$. This arrangement of the *L*-phase peaks is identical to that found for $\text{Hg}_{3-\delta}\text{AsF}_6$, and corresponds to the structure illustrated as Fig. 11 of Pouget *et al.* (1978).

(b) The host-lattice structure below T_c

Details of the Bragg intensity measurements at $T < T_c$ and the subsequent least-squares structure refinements are summarized in Table 1.

The crystal of $\text{Hg}_{3-\delta}\text{TaF}_6$ used for the low-temperature study was the same as that used for the structure determination at room temperature (Tun, Brown & Ummat, 1984) facilitating a direct comparison of the two. The $\text{Hg}_{3-\delta}\text{SbF}_6$ sample used in the present study was different from that used in the earlier room-temperature structure analysis (Tun & Brown, 1982) and had a concave side which made the absorption correction by numerical integration uncertain. In order to compare the low-temperature

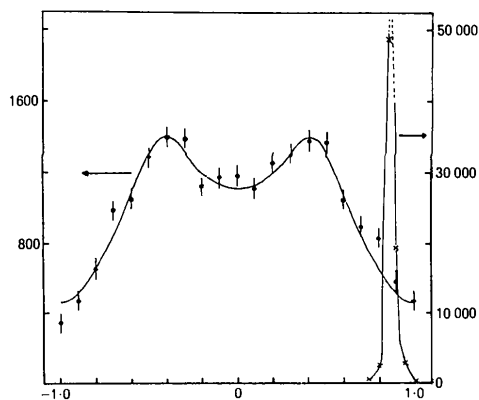


Fig. 1. Scan of the line $(3-\delta, m, 0)$ for $\text{Hg}_{3-\delta}\text{SbF}_6$ at 194 K (solid circles) and 164 K (crosses). Vertical circles are intensities (counts min^{-1}), horizontal scale gives m in units of \mathbf{a}_H^* .

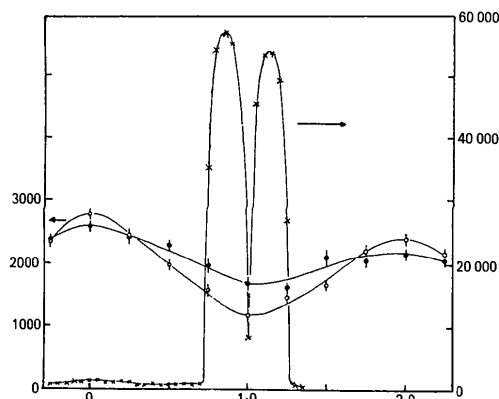


Fig. 2. Scan of the line $(3-\delta, m, 0)$ for $\text{Hg}_{3-\delta}\text{TaF}_6$ at 293 K (solid circles), 210 K (open circles) and 150 K (crosses). Horizontal scale as in Fig. 1. The vertical scales (intensities in counts min^{-1}) should not be compared as they refer to measurements made on two different crystals.

Table 1. *Summary of structure determination*

When three entries separated by semi-colons are shown the first two entries correspond to $M = \text{Sb}$ (293 and 173 K) and the last to $M = \text{Ta}$ (150 K) respectively.

Diffractometer: Nicolet P2₁

Cooling rate: $<1^\circ \text{ min}^{-1}$

Lattice constants determined from 15 well centred reflections having $10 < 2\theta < 26^\circ$; $10 < 2\theta < 52^\circ$; $9 < 2\theta < 27^\circ$

Data set (I) (includes at least one measurement of every non-equivalent reflection)

Maximum 2θ : 55°

$0 \leq h, k \leq 10, -16 \leq l \leq 16$

Number of reflections measured: 933; 907; 912

Number of unobserved reflections measured [$I < 3\sigma(I)$]: 455; 296; 142

Number of unique reflections: 253; 245; 246

Data set (II) (includes all equivalent reflections for selected large structure factors for testing absorption correction)

$-3 \leq h, k, l \leq 3$

Number of reflections measured: 144

Number of unique reflections: 14

Standard reflections: 015, 024; 015, 024; $\bar{4}20$, 008

E.s.d. of standard reflections (%): 2.3, 1.8; 2.1, 2.3; 2.0, 1.2

Number of standard reflection measurements: 25; 34; 21

Final $R = 0.057$; 0.058; 0.039 (all reflections)

Final $wR = 0.063$; 0.071; 0.045 (all reflections)

Weighting scheme: $w = [\sigma^2(\text{counting}) + k^2 F_o^2]^{-1}$ with $k = 0.0560$; 0.1100; 0.0425

Standard deviation of observation of unit weight: 0.89; 0.62; 1.03

Max. shift/e.s.d. in final cycle: 0.36; 0.54; 0.11

Av. shift/e.s.d. in final cycle: 0.03; 0.14; 0.02

Secondary-extinction correction (Larson, 1967): $g(\times 10^7) = 1.0(5)$; 2.4(7); 3.8(6)

Number of variables refined: 21; 21; 25

Residual electron density, max: $+1.5$; $+2.8$; $+6.3 \text{ e}\text{\AA}^{-3}$
min: -1.6 ; -3.0 ; $-1.9 \text{ e}\text{\AA}^{-3}$

structure with that at room temperature in this study we refined both the low-temperature and the room-temperature structures using data measured from the same crystal and using the same absorption correction. The resulting room-temperature refinement was not as good as that reported previously (Tun & Brown 1982) but was more suitable for comparison with the low-temperature structure. Because the Hg chains order into a lattice with monoclinic symmetry, the host-lattice symmetry must also be reduced from tetragonal to monoclinic below T_c but the distortion is too small to be measured. Consequently the structures are both reported in the tetragonal setting.

For each structure determination two sets of intensities, I and II, were measured (see Table 1). The former consists of all the non-systematically absent reflections with $2\theta \leq 55^\circ$ in one quadrant of reciprocal space while the latter contains all the equivalent reflections of selected strong Bragg peaks occurring at small 2θ . Data set II was measured in order to check the absorption correction but for $\text{Hg}_{3-\delta}\text{TaF}_6$ both data sets were averaged for the final refinements. Methods for applying the absorption

correction using numerical integration and details of the least-squares refinement procedure have been described in previous publications (see Tun & Brown, 1982; Tun *et al.*, 1984). The refined parameters are given in Table 2 along with the corresponding room-temperature parameters.*

Discussion

(a) *The S phase*

The *S* structure of the Hg chains in $\text{Hg}_{3-\delta}\text{SbF}_6$ is similar to that found for $\text{Hg}_{3-\delta}\text{AsF}_6$. The partial ordering between the parallel chains can be described in terms of two crystal domains of a body-centred monoclinic cell. In the first domain the Hg atoms in each chain are shifted with respect to those in the adjacent chain on the same layer (same z) by $(0.6 \pm \varepsilon)d_{\text{Hg}}$ (d_{Hg} = spacing between Hg atoms in the chain) while in the other domain the shift is $-(0.6 \pm \varepsilon)d_{\text{Hg}}$. The uncertainty ε , which is responsible for the q -dependent broadening of the *S*-phase peaks, was deduced from Fig. 1 to be $\pm 0.3d_{\text{Hg}}$.

The positions of the *S*-phase peaks of $\text{Hg}_{3-\delta}\text{TaF}_6$ correspond to a different ordering between the parallel chains. In this case, the Hg atoms in adjacent chains are not shifted with respect to each other and consequently they form an *A*-face-centred orthorhombic cell (or a monoclinic cell with a mean monoclinic angle $\gamma = 90^\circ$). Only one domain is required to explain the observed intensity modulation but the possibility of having two domains with γ slightly different from 90° cannot be excluded. The width of the $n=1$ peaks shown in Fig. 2 corresponds to $\varepsilon = \pm 0.5d_{\text{Hg}}$.

The parallel-chain interaction in $\text{Hg}_{3-\delta}\text{AsF}_6$ has been analysed by Emery & Axe (1978) using quasi-elastic neutron diffraction measurements. They obtained $\nu_2 \approx -2\nu_1 \approx 0.14 \text{ K}$ when ν_1 and ν_2 are nearest- and second-nearest-neighbour parallel-chain interactions (a positive interaction is repulsive). The interactions in $\text{Hg}_{3-\delta}\text{SbF}_6$ are qualitatively similar to the ones in $\text{Hg}_{3-\delta}\text{AsF}_6$ although the magnitudes of ν_1 and ν_2 are presumably smaller. The interaction in $\text{Hg}_{3-\delta}\text{TaF}_6$, on the other hand, is expected to be dominated by an attractive ν_1 (ν_2 could be attractive or weakly repulsive) since the parallel chains order to form *A*-face-centred cells.

(b) *The L phase*

The *L* phases of $\text{Hg}_{3-\delta}\text{SbF}_6$ and $\text{Hg}_{3-\delta}\text{TaF}_6$ are isostructural with the *L* phase of $\text{Hg}_{3-\delta}\text{AsF}_6$.

The bond lengths and other important distances in the *L* phase of $\text{Hg}_{3-\delta}\text{SbF}_6$ and $\text{Hg}_{3-\delta}\text{TaF}_6$, mostly

* Details of all absorption corrections are given by Tun (1985a) and lists of observed and calculated structure factors have been given by Tun (1985b).

Table 2. Atomic parameters

The first two entries correspond to $M = \text{Sb}$ (293 and 173 K) and the last two to $M = \text{Ta}$ (293 and 150 K), respectively. The parameters for $M = \text{Ta}$ (293 K) are taken from Tun *et al.* (1984).

	x	y	z	U_{11}^*	U_{22}	U_{33}	U_{12}	U_{13}	U_{23}
Hg(1)†	0	1/32	-0.0010 (10)	57 (1)					
	0	1/32	-0.0013 (5)	29 (1)					
	0	1/32	-0.0007 (5)	57 (1)	56	57 (2)	0	0	0
	0	1/32	-0.0016 (4)	23 (1)	24	25 (2)	0	0	0
Hg(2)†	0	3/32	-0.0006 (8)	55 (1)					
	0	3/32	-0.0003 (4)	28 (1)					
	0	3/32	-0.0009 (4)	56 (2)	55	55 (2)	0	0	0
	0	3/32	-0.0010 (4)	24 (2)	24	24 (2)	0	0	0
Hg(3)†	0	5/32	0.0019 (6)	51 (1)					
	0	5/32	0.0015 (4)	26 (1)					
	0	5/32	0.0014 (4)	57 (2)	53	49 (2)	0	0	0
	0	5/32	0.0010 (3)	23 (2)	23	23 (2)	0	0	0
Hg(4)†	0	7/32	0.0025 (4)	50 (1)					
	0	7/32	0.0028 (3)	26 (1)					
	0	7/32	0.0023 (2)	57 (1)	52	47 (1)	0	0	0
	0	7/32	0.0024 (2)	25 (1)	22	19 (1)	0	0	0
Sb	0	1/4	3/8	33 (2)	U_{11}	25 (1)	0	0	0
Sb	0	1/4	3/8	16 (2)	U_{11}	11 (1)	0	0	0
Ta	0	1/4	3/8	34 (1)	U_{11}	25 (1)	0	0	0
Ta	0	1/4	3/8	13 (1)	U_{11}	12 (1)	0	0	0
F(1)	0	1/4	0.2302 (13)	45 (11)	108 (18)	36 (8)	0	0	0
	0	1/4	0.2267 (12)	43 (11)	36 (10)	19 (7)	0	0	0
	0	1/4	0.2268 (9)	56 (7)	151 (14)	30 (5)	0	0	0
	0	1/4	0.2253 (11)	16 (7)	74 (13)	15 (6)	0	0	0
F(2)	0.672 (2)	$x+1/4$	7/8	46 (7)	U_{11}	78 (9)	-7 (5)	$-U_{23}$	-4 (10)
	0.673 (2)	$x+1/4$	7/8	27 (6)	U_{11}	35 (6)	-4 (4)	$-U_{23}$	7 (8)
	0.673 (1)	$x+1/4$	7/8	50 (4)	U_{11}	89 (6)	-11 (3)	$-U_{23}$	5 (7)
	0.675 (1)	$x+1/4$	7/8	19 (4)	U_{11}	20 (4)	-5 (3)	$-U_{23}$	3 (6)

* In Å^2 ; $U_{11} = U_{\text{iso}}$ for the Hg atoms of $\text{Hg}_{3-\delta}\text{SbF}_6$ structures, otherwise temperature factors are given in the form $\exp(-2\pi^2 \sum 10^{-4} U_{ij} H_i H_j a_i^* a_j^*)$.
 † Partial Hg atoms placed at regular intervals along y to simulate the incommensurate chains.

Table 3. Bond lengths and important distances (Å) in $\text{Hg}_{3-\delta}\text{MF}_6$ ($M = \text{Sb}, \text{Ta}$) compounds

	$\text{Hg}_{3-\delta}\text{SbF}_6$ (293 K)	$\text{Hg}_{3-\delta}\text{SbF}_6$ (173 K)	$\text{Hg}_{3-\delta}\text{TaF}_6$ ¶ (293 K)	$\text{Hg}_{3-\delta}\text{TaF}_6$ (150 K)
$M-F(1)(\times 2)$	1.83 (2)	1.86 (2)	1.88 (1)	1.89 (2)
$M-F(2)(\times 4)$	1.88 (2)	1.87 (1)	1.884 (6)	1.893 (8)
Hg-Hg (interchain)*	2.66 (2)	2.671 (1)	2.674 (4)	2.671 (1)
u_0 †	0.032 (5)	0.035 (4)	0.030 (3)	0.030 (3)
Chain-chain‡	3.22 (1)	3.210 (8)	3.239 (6)	3.213 (6)
F(1)-chain§	2.88 (1)	2.81 (1)	2.86 (1)	2.81 (1)
F(2)-chain§	2.98 (1)	2.956 (6)	2.983 (4)	2.937 (5)

* Room-temperature values were calculated from the spacing between the diffuse scattering sheets on precession photographs. Low-temperature values were determined by the diffractometer using at least four well centred Bragg peaks arising from the ordered Hg chains.

† Maximum displacement (Å) of the chain from the straight configuration.

‡ The closest contact distance between the two neighbouring perpendicular chains which is greater than $c/4$ by $2u_0$.

§ Shortest distance to the neighbouring chain.

¶ Taken from Tun *et al.* (1984).

obtained from the least-squares structure refinements using the host-lattice Bragg reflections, are listed in Table 3. The low-temperature Hg-Hg intrachain spacing is 2.617 Å in both compounds and equal to the room-temperature spacings within experimental error, indicating that the thermal expansion of the chain is very small as noted also for $\text{Hg}_{3-\delta}\text{AsF}_6$ by Pouget *et al.* (1978).

In spite of the ordering of the chains there are very few changes in the host lattice below T_c . As the $M-F$ bonds do not change significantly with temperature

the thermal contraction of the host lattice is mainly caused by the contraction in the chain-chain and F-chain distances, in agreement with Khan's (1976) observation that only bonds with small bond valence show a significant coefficient of thermal expansion. The unusual feature of these compounds is that the chains and the host lattice are free to expand independently giving rise to changes in δ and hence apparent changes in the chemical composition at different temperatures, an effect that has been related to the appearance of elemental mercury on the crystal sur-

faces on cooling (Datars, van Schyndel, Lass, Chartier & Gillespie, 1978).

The r.m.s. atomic displacement parameters (U) of the F atoms show a large anisotropy. In particular, $U_{22} \gg U_{11}$ for F(1) and $U_{33} > U_{11}$ for F(2) in all the room-temperature structures. This feature was attributed by Tun & Brown (1982) to an artifact of a static rotational disorder of the MF_6 ion induced by the variable position of the Hg atoms in the adjacent chain. Since the chains and the host lattice remain incommensurate even at $T < T_c$, only a small change in U_{22} of F(1) and U_{33} of F(2) with temperature was then expected. However, the large ratios of displacement parameters observed [$\langle U(173 \text{ K})/U(293 \text{ K}) \rangle = 0.50$ for $Hg_{3-\delta}SbF_6$ and $\langle U(150 \text{ K})/U(293 \text{ K}) \rangle = 0.43$ for $Hg_{3-\delta}TaF_6$] are roughly proportional to the ratios of the temperatures of measurement (0.59 and 0.51 respectively) suggesting that the anisotropies in the r.m.s. displacements of the F atoms at room temperature are dynamic and presumably are coupled to the thermal sliding modes of the chains.

The competition between parallel and perpendicular coupling

The L phase is produced by a direct repulsion between the atoms in neighbouring perpendicular chains and results in a structure in which the Hg atoms avoid each other at the crossing points. The distance between chains is about 3.24 \AA (at 293 K) in all three structures, $Hg_{3-\delta}AsF_6$, $Hg_{3-\delta}SbF_6$ and $Hg_{3-\delta}TaF_6$, so that the strength of the interaction is probably similar and results in the distance between nearest-neighbour Hg atoms in perpendicular chains ranging between 3.34 and 3.47 \AA . On the other hand, the

interaction between parallel chains which is mediated by the host lattice will change as the anion becomes larger. The effect of this can be seen in the poorer ordering in the S phase of the Sb and Ta compounds compared to As and the higher temperature at which the transition to the L phase occurs.

We wish to thank the Natural Sciences and Engineering Research Council of Canada for an operating grant and Brookhaven National Laboratory for assistance in the measurement of T_c for $Hg_{3-\delta}SbF_6$.

References

- AXE, J. D. (1980). In *Ordering in Strongly Fluctuating Condensed Matter Systems*, edited by T. RISTE. New York: Plenum.
- BROWN, I. D., CUTFORTH, B. D., DAVIES, C. G., GILLESPIE, R. J., IRELAND, P. R. & VEKRIS, J. E. (1974). *Can. J. Chem.* **52**, 791–793.
- DATARS, W. R., VAN SCHYNDEL, A., LASS, J. S., CHARTIER, D. & GILLESPIE, R. J. (1978). *Phys. Rev. Lett.* **40**, 1184–1187.
- EMERY, V. J. & AXE, J. D. (1978). *Phys. Rev. Lett.* **40**, 1507–1511.
- HASTINGS, J. M., POUGET, J. P., SHIRANE, G., HEEGER, A. J., MIRO, N. D. & MACDIARMID, A. G. (1977). *Phys. Rev. Lett.* **39**, 1484–1487.
- KHAN, A. A. (1976). *Acta Cryst.* **A32**, 11–16.
- LARSON, A. C. (1967). *Acta Cryst.* **23**, 664–665.
- POUGET, J. P., SHIRANE, G., HASTINGS, J. M., HEEGER, A. J., MIRO, N. D. & MACDIARMID, A. G. (1978). *Phys. Rev. B*, **18**, 3645–3656.
- SPAL, R., CHEN, C. E., EGAMI, T., NIGREY, P. J. & HEEGER, A. J. (1980). *Phys. Rev. B*, **21**, 3110–3118.
- TUN, Z. (1985a). PhD thesis (Appendix), McMaster Univ., Hamilton, Ontario, Canada L8S 4M1.
- TUN, Z. (1985b). PhD thesis, Table 1, available from the Thode Library, McMaster Univ., Hamilton, Ontario, Canada L8S 4M1.
- TUN, Z. & BROWN, I. D. (1982). *Acta Cryst.* **B38**, 2321–2324.
- TUN, Z., BROWN, I. D. & UMMAT, P. K. (1984). *Acta Cryst.* **C40**, 1301–1303.

Acta Cryst. (1986). **B42**, 213–224

On the Prediction of Structure Changes in Bi_2O_3 Caused by Ordering and Pseudo-Jahn–Teller Instability

BY KARIN KHACHATURYAN

Nov. Cheremushka 32a, B15-Apt 40, Moscow 113461, USSR

(Received 22 July 1985; accepted 14 August 1985)

Abstract

The structures of the β and δ phases of Bi_2O_3 are predicted theoretically. The concentration-wave method is used to determine the oxygen ordering over tetrahedral interstices of the f.c.c. Bi host. This method yields two modifications for the δ phase. One is a disordered phase in which O atoms randomly

occupy tetrahedral interstices of the f.c.c. host. This structure agrees with the model proposed by Gattow & Schröder [*Z. Anorg. Allg. Chem.* (1962), **318**, 176–189]. The second modification is the interstitial superstructure in which O atoms are regularly distributed over tetrahedral sites. Its structure agrees with the Sillen model [Sillen (1937). *Ark Kemi Mineral. Geol.* **12A**, 1–15]. It is shown that the structure of the β